

TECH. MEMO
RAD-NAV 32

UNLIMITED

BR52294

TECH. MEMO
RAD-NAV 32

(1)

ROYAL AIRCRAFT ESTABLISHMENT

ADA033372

MICROWAVE LANDING SYSTEM ACCURACY REQUIREMENTS
FOR AUTOMATIC FLARE-OUT

by

P. W. James

March 1976

DISTRIBUTION STATEMENT A
Approved for public release
Distribution Unlimited

COPYRIGHT ©

CONTROLLER HMSO LONDON
1976

DDC
RECEIVED
DEC 3 1976
RECEIVED
A D

© Crown copyright 1976

UNLIMITED

DISTRIBUTION FOR	
W710	Write Section <input checked="" type="checkbox"/>
010	Buff Section <input type="checkbox"/>
020	<input type="checkbox"/>
DATE: 10/3/76	
BY: [Signature]	
REMARKS: [Blank]	

- 1 -

ROYAL AIRCRAFT ESTABLISHMENT

⑨ Technical Memorandum, Rad-Nav 32

Received for printing 10 March 1976

⑥ MICROWAVE LANDING SYSTEM ACCURACY REQUIREMENTS
FOR AUTOMATIC FLARE-OUT.

by

⑩ P. W. James

⑪ Mar 76

⑫ 39 p.

SUMMARY

The report describes adaptation of a computer based simulation of a transport aircraft automatic landing system to enable study of microwave landing system (MLS) flare guidance. The simulation was used to examine the allowable errors from the range and elevation angle measuring sub-systems of the MLS flare system.

⑭ RAE-TM-Rad-Nav-32

⑮ DRIC

⑯ BR-52294

DDC
RECEIVED
DEC 2 1976
RECEIVED
D

310 450
HB

1 INTRODUCTION

The operational requirement for the ICAO 'new non-visual precision approach and landing guidance system' requires that elevation guidance shall be provided for the flare-out phase of an automatic landing. The microwave landing systems (MLS) being developed to meet the ICAO requirement generally offer flare guidance by means of elevation angle guidance relative to a transmitter (elevation No.2) located some 450m upwind of the origin of the glidepath transmitter (elevation No.1). Derivations of height in the flare-out region is achieved by combining range information with elevation No.2 angle information. Range information is obtained from an MLS ranging sub-system, probably located at the upwind end of the runway, but possibly elsewhere, e.g., co-located with the elevation No.2 transmitter.

The accuracy requirement for the MLS range and elevation No.2 angle information is as yet ill-defined and there is likely to be a sensitive relationship between guidance system cost and accuracy. In particular, relaxation of the 3 to 6m accuracy target, which has so far been used for MLS ranging sub-system development, might allow substantial economies to be realised, through building the ranging system at L-band, rather than C-band.

This simulation study, described in this paper, has therefore been performed to provide some guidance as to MLS ranging and angle sub-system accuracy requirements for automatic flare-out. At this stage in the UK MLS programme, the detailed error characteristics of MLS elevation No.2 and ranging systems are unknown and it has therefore been necessary to make arbitrary assumptions as to the nature of the errors. The philosophy which has been adopted is as follows. A selection of error profiles (step, sequence of steps, random) has been made and for each type of error, that error timing relative to the flare-out manoeuvre has been determined which produces the maximum change in touchdown performance (rate of descent and range). A proportion of the allowable normal touchdown error variance has been allocated to the effects of ranging system and angle system errors and the maximum allowable amplitude of the 'worst case' error of each class has been determined. These 'worst case' errors are proposed as guidelines for system design. Tests have been made to examine whether guidance errors which induced acceptable touchdown errors could result in elevator activity unacceptable to the human pilot.

2 SYSTEM GUIDANCE GEOMETRY

The airfield layout used for the simulation is shown in plan in Fig.1 and in elevation in Fig.2.

It was convenient to take as origin of co-ordinates the point at which the runway intercepted the asymptote to a 3deg glide path. This point was 300m (984ft) from threshold. The height of the centre of the elevation No.1 array was 2.74m (9ft), and so it was positioned $2.74 \cot 3\text{deg}$ or 52.3m (172ft) downwind of the origin. The lateral offset from the runway centre line was 150m (492ft) for both the elevation No.1 and elevation No.2 arrays. The height to the centre of the elevation No.2 array was 3.66m (12ft), and this element was placed 450m (1476ft) upwind of the origin.

3 AIRCRAFT AND AFCS SIMULATION

A computer program was supplied by K. Watling, of BLEU, which simulated the approach and landing of a BAC 1-11 510 series aircraft fitted with an Elliott E2200 flight control system, deriving guidance from the ILS localiser and glide path and from a radio altimeter.

The following outline of the mode of operation of the AFCS may help in the understanding of later results.

During the approach, the elevator is controlled in a loop which tries to maintain the ILS glide path deviation at zero. The throttle is controlled in a second loop which attempts to maintain a constant air speed. At height 200ft, as indicated by the radio altimeter, the gain of the angular guidance loop is halved, to prevent the loop gain becoming too high at the short range. When the radio altimeter indicates 100ft, the angular guidance is disconnected, and the elevator control loop then tries to keep a constant attitude. At 50ft on the radio altimeter, the flare is initiated. The thrust demand is reduced linearly with time until a certain minimum value is reached and then held constant. The elevator loop receives height and height rate inputs and causes the aircraft to execute an approximately exponential flare, touching down with a vertical speed of about 0.6m/s (2ft/s).

Since the AFCS derives height rate from raw radio altitude, it is likely to be more sensitive to guidance errors than possible future flight control systems using inertially smoothed height rate.

4 PROGRAM MODIFICATION FOR MLS SIMULATION

4.1 After converting the original program to 1900 ALGOL it was tested for a typical case with a 3deg ILS approach at a speed of 125kn (211.3ft/s) and a wind speed of 12kn (20ft/s). The attitude at touch-down was noted (3.72deg).

4.2 The program was then modified so that the original ILS signal was replaced by the elevation No.1 MLS signal and the radio altimeter output was replaced by the combination of elevation No.2 and distance measurement.

It was assumed that the MLS antennas for all three functions were located on the aircraft nose at the point shown in Fig.3. This point was 12.9m (42.2ft) ahead of the centre of gravity and 1.9m (6.1ft) above the wheels when in a nominal approach attitude. For an attitude θ rad we have, approximately

$$\text{antenna height} = \text{wheel height} + 1.9 + 12.9\theta \quad \text{m.} \quad (1)$$

The angle measured by the elevation No.1 system is given as a function of antenna height and the range of the aircraft CG to the asymptotic glide path intercept by

$$\text{elevation No.1} = \arctan \left\{ \frac{\text{antenna height} - 2.7}{\sqrt{[(\text{range} - 12.9 - 52.4)^2 + 150^2]}} \right\}. \quad (2)$$

With all angles expressed in degrees, the quantity replacing the original ILS angular error is just

$$\text{elevation No.1} - 3 \quad (3)$$

Note that formula (2) assumes that the aircraft antenna remains in the vertical plane containing the runway centre line.

The elevation No.2 angle is given by

$$\text{elevation No.2} = \arctan \left\{ \frac{\text{antenna height} - 3.66}{\sqrt{[(\text{range} - 12.9 + 450)^2 + 150^2]}} \right\}. \quad (4)$$

For range measurement from a site at the far end of the runway, we assume that, by subtracting a constant, the distance^(O) is available measured to the perpendicular from the elevation No.2 site on to the runway, giving

$$\text{distance } O = \text{range} + 450. \quad (5)$$

The ^{true} time distance from the elevation No.2 site will be denoted by distance No.2, which is given by

$$\text{distance No.2} = \sqrt{[(\text{range} - 12.9 + 450)^2 + 150^2]}. \quad (6)$$

If distance No.2 is known to the aircraft, it could compute the height of its antenna as:

$$\text{distance No.2} \times \tan (\text{elevation No.2}) + 3.66.$$

However in this Memo we assume that it is distance 0 that is measured, and this is used instead of distance No.2. Thus the actual expression for the aircraft height as if measured by the radio altimeter is:

$$\begin{aligned} &(\text{distance } 0) \times \tan (\text{elevation No.2}) \\ &+ 3.66 - 1.86 - (12.9 - 8.2) \times 3.72/57.3 \quad \text{m. (7)} \end{aligned}$$

Here we have allowed for:

- (a) antenna height 1.86m (6.1ft) above wheels in datum attitude;
- (b) antenna 12.9m (42.2ft) forward of CG;
- (c) radio altimeter 8.2m (27ft) forward of CG; and
- (d) touch-down attitude 3.72deg.

Figs.4 to 7 show the results of a simulated MLS approach and landing. The run was started at a wheel height of 91m (300ft), a speed of 125kn (211ft/s, 64.4m/s) and with the MLS antenna following the asymptote 3deg glide path. The wind speed was 12kn (20ft/s, 6m/s).

The slight perturbation at the beginning of the run, most visible on the curve for elevation deflection, is due to the fact that the hyperbolic glide path is slightly above the asymptote. The aircraft is obliged to climb a small distance to acquire the hyperbolic path. There is another small perturbation at 61m (200ft) height due to the gain switching.

Touch-down occurred at 194m (637ft) from the intersection point with an airspeed of 116kn (196ft/s, 50m/s), a descent speed of 0.53m/s (1.74ft/s) and an attitude of 3.8deg, values sufficiently close for our purposes to those obtained with radio altimeter flare guidance.

5 THE EFFECTS OF STEP ERRORS IN DISTANCE AND ELEVATION NO.2 MEASUREMENTS

Approaches and landings were simulated in which an error of fixed amount was introduced into the distance measurement when the aircraft was below a given height. In Figs.8 and 9 are shown the change in touch-down vertical speed and the change in touch-down position, plotted as functions of the height below which the errors were introduced. The values of the distance error, between -160 and 160ft, are given as parameters to the curves.

The most conspicuous feature of these curves is the rapid changes around 50ft height. This is the height at which the flare begins. The data contained in these curves have been used to derive maximum allowable MLS and range information errors, as described in section 6 below and in the Appendix.

Figs.10 and 11 show the corresponding effects of step errors introduced into the elevation No.2 angles. In this case we show curves only for errors of ± 0.01 deg.

6 WORST CASES FOR RANGE AND ELEVATION ERRORS

6.1 We are interested in finding out how great the range and elevation errors can be before the variations in touch-down vertical velocity and position become unacceptable. Guided by ARB paper No.367¹, which assigns standard deviations of 0.46m/s (1.5ft/s) and 90m (295ft) respectively in these quantities, we shall assume that the guidance system should not contribute more than 40% of the total variance and that of that 40%, the ranging sub-system can contribute one quarter and the angle sub-system three quarters. This ratio is intended to recognise the technical difficulty of providing precise angle guidance at low elevation angles. This then leads to the following maximum allowable standard deviations of touch-down parameters due to worst case range and angle system errors.

Table 1

	Vertical velocity m/s (ft/s)	Position m (ft)
Ranging system	0.14 (0.47)	28 (93)
Angle system	0.25 (0.82)	49 (162)

It should be noted that it is more common in other spheres of approach and landing guidance to allocate half the total allowable variance to the guidance system errors. However, in the case of flare guidance, the radio altimeter has provided a precedent of very high guidance quality over the runway and it is felt desirable that MLS flare guidance quality should be constrained to approach that of radio altimeter guidance. Hence the reduced allocation of variance (40%) to MLS flare guidance.

We now compute the largest allowable errors in range and elevation such that the above changes in touch-down parameters are not exceeded. The methods are given in the Appendix, and use data from section 5. The sensitivity functions were derived from the simulations described above, and some are shown in Figs.17 to 20.

The results depend on whether the errors are random or deterministic, and also on how they vary along the aircraft path. A wide range of possibilities could be considered, but we have restricted attention to single step errors, sequences of steps of equal amplitude and random errors of unspecified spectrum. The results are summarised below.

6.2 Deterministic errors

6.2.1 Single step

The error is assumed zero up to a certain point, at which it suddenly changes to a new value and remains constant. The maximum allowable errors are given in Table 2.

Table 2

	Step amplitude for 1 sd change	
	In vertical velocity	In range
Range error m (ft)	43.8 (144)	39.6 (130)
Angle error deg (mrad)	0.0571 (0.996)	0.0398 (0.695)

For example, if the step in range error were 43.8m, it would cause a change in touch-down vertical velocity of 0.14m/s as in Table 1.

6.2.2 Step sequence

The errors are permitted to have any value at every point, such that the error magnitude does not exceed a limiting value. In the worst case the error will be equal to this limiting value multiplied by ± 1 . Table 3 shows the values of this magnitude in the four cases.

Table 3

	Error magnitude limit for not more than 1 sd change	
	In vertical velocity	In range
Range error m (ft)	16.4 (53.8)	15.2 (49.9)
Angle error deg (mrad)	0.0190 (0.332)	0.0202 (0.353)

For example, if the angular error was 0.0202deg at every point, and the direction of the error was in the more unfortunate sense so that their effects added, then the change in touch-down range would be $\pm 49\text{m}$.

6.3 Random errors

In this case we assume that the error at each point is random with a mean and a standard deviation. These quantities need not be the same at all points. In fact we do not assume the errors are stationary, nor do we make any assumptions about their distribution or correlations. The mean can be regarded as a deterministic error, of which examples have been considered above, so we restrict attention to the case of zero mean error.

The upper bounds for the standard deviations of range and elevation measurements are shown in Table 4.

Table 4

	Standard deviation limit for 1 sd change in	
	Vertical velocity	Range
Range error m (ft)	85.4 (280)	44.6 (146)
Angle error deg (mrad)	0.0465 (0.812)	0.0774 (1.35)

For example, if the standard deviation of range error at any point along the path was 44.6m or less, then we can be sure that the standard deviation of touch-down vertical velocity was *at most* 0.14m.

6.4 It is concluded from this preliminary series of tests that, assuming the worst possible 'noise' characteristics of the ranging and flare angle measurement systems, range errors of 15m (50ft) standard deviation and angle errors of 0.02deg standard deviation should be acceptable.

It must be noted that these errors are derived from a simple study of the effects of the errors on otherwise unperturbed flare-out manoeuvres. Examination of detailed touch-down error distributions in the presence of turbulence, wind shear, etc., may require some revision of the detailed numbers for specific systems.

7 TRANSIENT MOTIONS OF THE ELEVATOR FOLLOWING A STEP ERROR IN RANGE

Since sudden large elevator movements would be unacceptable to the pilot, it is of interest to exhibit the motion of the elevator following a step error of the kinds previously used. Simulations were performed in which an error of 30m (100ft) in the range measurement was introduced below heights of 45, 35, 25, 15 and 5ft. Figs.12 to 16 show the resultant elevator motions (with the unperturbed case shown dotted).

We see that the maximum motions are about ± 2 deg for the 45ft case, and less for the other cases.

Since the maximum allowable range information error is 15m (50ft) (1 sd), (section 6) we may conclude that elevator activity from this cause will generally be less than 1deg (1 sd). Practical MLS ranging systems are aiming at accuracies of 6m (20ft) (1 sd) and assuming a tentative limit of acceptable activity as 1deg (1 sd), problems due to elevator activity from this source are unlikely. However, since the flare elevation angle information is allowed to have a larger effect than range error on the touch-down parameters, it is likely that there will be elevator activity problems from elevation angle guidance errors. These will require detailed study when actual flare elevation error data are available.

8 CONCLUSIONS

In the absence of detailed information on the noise and bias characteristics of practical MLS flare guidance systems, allowable values of range and angle error have been derived on the assumption that the errors could be in the

form of a single step, a sequence of steps or any arbitrary random process. Errors in the form of a sequence of steps have been found to have the greatest effect on the aircraft/autopilot combination studied (BAC 1-11 500 series and Elliott E2200 AFCS). Assuming an error of this form, range errors of 15m (1 sd) and elevation angle errors of 0.02deg (1 sd) appears acceptable.

In assessing the effects of errors attention has primarily been directed to achieving acceptable performance in range and rate of descent at touch-down. Elevator activity has also been briefly examined, and while practical values of range error are unlikely to have a significant effect, elevator activity will need to be studied in greater detail when practical MLS flare elevation data are available.

REFERENCE

<u>No.</u>	<u>Author</u>	<u>Title, etc.</u>
1	Air Registration Board	British civil airworthiness requirements. Paper No.367, issue 3 (1970)

AppendixA.1 Definition of sensitivity

Consider the change v of a variable V due to errors in a measurement M . For example, V could be touch-down descent speed and M an angle of elevation. The error in M will be denoted by $m(x)$, describing the error as a function of position along the aircraft path, x being a parameter such as time, distance or height.

We assume the effect of m is determinate, so v is a function of the function m . For an arbitrary m and a constant λ , we assume that

$$v(\lambda m) = \int_a^b S(x) \lambda m(x) dx + O(\lambda^2) \quad \text{as } \lambda \rightarrow 0 \quad (\text{A-1})$$

where $[a, b]$ is the interval in x , and $S(x)$ is the *sensitivity of V to error in M at point x* . Equation (A-1) may be justified by Taylor's theorem, provided that there are no hard non-linearities effective at arbitrarily small perturbations.

It is convenient to define \tilde{v} to be the 'linearised' change in V , by

$$\tilde{v}(m) = \int_a^b S(x) m(x) dx . \quad (\text{A-2})$$

Hence a unit error existing over a short interval x to $x + dx$ will cause

$$\tilde{v} = S(x) dx .$$

A.2 Response to step errors

If the error in m is zero up to some value of x and 1 thereafter, that is,

$$m(x) = \begin{cases} 0 & (x < x_1) \\ 1 & (x \geq x_1) \end{cases}$$

then the linearised change in V will be denoted by $T(x_1)$, and is given by

$$T(x_1) = \int_x^b S(x) dx . \quad (A-3)$$

It follows that

$$S(x) = -T'(x) . \quad (A-4)$$

A.3 Worst case for errors of bounded magnitude

We now ask for the maximum value of v when $m(x)$ is subject to an upper bound on its magnitude, of say, unity.

It is obvious from (A-2) that for each x we should choose $m(x) = 1$ if $S(x) > 0$ and $m(x) = -1$ if $S(x) < 0$. Hence

$$m(x) = \operatorname{sgn}[S(x)] = \operatorname{sgn}[-T'(x)] .$$

This is a rectangular function with changeover points at the zeros of S , which are the extrema of T , say x_1, x_2, \dots, x_n (see Fig.21c).

The value of \tilde{v} is

$$\begin{aligned} \int_a^b S(x) \operatorname{sgn} S(x) dx &= \int_a^b |S(x)| dx \\ &= |T(a) - T(x_1)| + |T(x_1) - T(x_2)| + \dots + |T(x_n) - T(b)| \\ &\dots\dots\dots (A-5) \end{aligned}$$

the sum of the differences between successive extrema of T .

A.4 Worst case for a constant error existing over a continuous interval

Here we consider

$$m(x) = \begin{cases} 1 \\ 0 \end{cases} , \quad \begin{matrix} p \leq x \leq q \\ \text{otherwise} \end{matrix} .$$

The change in V is then

$$\int_p^q S(x)dx = T(p) - T(q) . \quad (A-6)$$

To maximise the magnitude of this, we choose p and q to correspond to the overall maximum and minimum of T . These will occur in the set $(a, x_1, x_2, \dots, x_n, b)$; in Fig.21 they happen to be x_1 and b , so the worst error will be from x_1 to b and will give

$$|\tilde{v}| = |T(x_1) - T(b)| .$$

The error function is shown in Fig.21d.

A.5 Random errors

In this and following sections, m will be taken to be a random function. Taking ensemble averages of (A-2)

$$\langle \tilde{v} \rangle = \int_a^b S(x) \langle m(x) \rangle dx . \quad (A-7)$$

Thus the average \tilde{v} depends on the ensemble mean of $m(x)$ just as for a determinate error.

Turning now to the variance of \tilde{v} , this is

$$\begin{aligned} D^2(\tilde{v}) &= \langle (\tilde{v} - \langle \tilde{v} \rangle)^2 \rangle \\ &= \int_a^b \int_a^b S(x) S(y) R(x, y) dx dy \end{aligned} \quad (A-8)$$

where $R(x, y)$ is the covariance

$$\langle [m(x) - \langle m(x) \rangle] [m(y) - \langle m(y) \rangle] \rangle , \quad x, y \in [a, b] \quad (A-9)$$

In particular the standard deviation of $m(x)$ is $\sigma(x)$ where

$$\sigma(x) = R(x, x)^{1/2} . \quad (A-10)$$

A.6 Worst case for unrestricted covariance

The covariance must always satisfy

$$|R(x,y)| \leq \sigma(x)\sigma(y) , \quad \text{all } x,y.$$

Hence

$$\begin{aligned} D^2(v) &\leq \int_a^b \int_a^b |S(x)S(y)R(x,y)| dx dy \\ &= \int_a^b \int_a^b |S(x)| |S(y)| |R(x,y)| dx dy \\ &\leq \int_a^b \int_a^b |S(x)| |S(y)| \sigma(x)\sigma(y) dx dy \\ &= \int_a^b |S(x)| \sigma(x) dx \int_a^b |S(y)| \sigma(y) dy \\ &= \left| \int_a^b |S(x)| \sigma(x) dx \right|^2 \end{aligned}$$

so

$$D(\tilde{v}) \leq \int_a^b |S(x)| \sigma(x) dx . \quad (A-11)$$

Now consider the case when

$$m(x) = \mu S(x) + \langle m(x) \rangle$$

where μ is a random variable with mean 0 and finite variance. For this case

$$R(x,y) = \langle \mu S(x) \mu S(y) \rangle = D^2(\mu) S(x) S(y)$$

$$\sigma(x) = R(x,x)^{\frac{1}{2}} = D(\mu) |S(x)|$$

and it is easy to verify that

$$D(\tilde{v}) = D(\mu) \int_a^b S(x)^2 dx = \int_a^b |S(x)| \sigma(x) dx .$$

Thus equality is attained in (A-11) when $m - \langle m \rangle$ is a random multiple of S , and so this is the worst possible case when the form of the covariance function is not specified.

Further

$$D(m) = D(\mu) |S(x)| \leq D(\mu) \max_x |S(x)| \leq \frac{D(\tilde{v}) \max_x |S(x)|}{\int_a^b |S(x)|^2 dx} .$$

A.7 Worst case for errors with stationary statistics

If the error function is stationary in the sense that $R(x,y)$ depends only upon the difference $x-y$, then we can introduce the power spectral density $P(\omega)$, related to R by

$$\left. \begin{aligned} P(\omega) &= \frac{1}{2\pi} \int_{-\infty}^{\infty} R(u) e^{-i\omega u} du \geq 0 \\ R(u) &= \int_{-\infty}^{\infty} P(\omega) e^{i\omega u} d\omega \end{aligned} \right\} \quad (A-12)$$

Here u has been written for $x-y$, and the ranges of integration are $-\infty$ to ∞ , the error functions m being supposed to be segments from samples of unlimited length. The variance of m is

$$\sigma^2(x) = R(x,x) = R(0) = \int_{-\infty}^{\infty} P(\omega) d\omega = 2 \int_0^{\infty} P(\omega) d\omega .$$

The variance of \tilde{v} is

$$\begin{aligned}
D^2(\tilde{v}) &= \int_a^b \int_a^b S(x)S(y) \int_{-\infty}^{\infty} P(\omega) \exp i\omega(x-y) d\omega dx dy \\
&= \int_{-\infty}^{\infty} P(\omega) \int_a^b S(x) e^{i\omega x} dx \int_a^b S(y) e^{-i\omega y} dy d\omega \\
&= \int_{-\infty}^{\infty} P(\omega) \left| \int_a^b S(x) e^{i\omega x} dx \right|^2 d\omega \\
&= 2 \int_0^{\infty} P(\omega) \left| \int_a^b S(x) e^{i\omega x} dx \right|^2 d\omega . \tag{A-13}
\end{aligned}$$

For a given variance σ^2 of m , this quantity is maximum when $P(\omega)$ zero everywhere except for the value of ω which maximise $\left| \int_a^b S(x) e^{i\omega x} dx \right|$, say ω_{\max} ; i.e.

$$P(\omega) = \frac{1}{2} \sigma^2 \delta(\omega - \omega_{\max}) .$$

This gives

$$D^2(\tilde{v}) = \sigma^2 \max_{\omega} \left| \int_a^b S(x) e^{i\omega x} dx \right|^2 . \tag{A-14}$$

The worst stationary noise case consists of narrow band noise at the most sensitive frequency.

A.8 Uniform power spectrum

In the special case when $P(\omega)$ is a constant, say P (m-units)² per (radian/x-unit) we get a variance

$$D^2(\tilde{v}) = 2P \int_0^{\infty} \left| \int_a^b S(x) e^{i\omega x} dx \right|^2 d\omega . \tag{A-15}$$

Of course, $P(\omega) = \text{constant}$ is impossible since it would lead to an infinite variance, but we can suppose it constant over all x where $\int_a^b S(x) e^{i\omega x} dx$ is significant.

Then

$$\begin{aligned}
 D^2(\tilde{v}) &= 2P \int_0^\infty \int_a^b \int_a^b S(x)S(y)e^{i\omega(x-y)} dx dy d\omega \\
 &= 2P \int_a^b \int_a^b S(x)S(y)\pi\delta(x-y) dx dy \\
 &= 2P\pi \int_a^b S(x)^2 dx \\
 &= \int_a^b S(x)^2 dx \times [\text{noise power, in m-units squared per (cycle per x unit)}] \\
 &\dots\dots (A-16)
 \end{aligned}$$

A.9 Sampled data

We suppose that the measurement M is performed at discrete instances x_i , separated by Δx .

We assume each measurement m_i is extended in box-car fashion to length Δx . Then

$$\tilde{v} = \sum_i S(x_i)m_i\Delta x \quad (A-17)$$

The mean is

$$\langle \tilde{v} \rangle = \sum_i S(x_i)\langle m_i \rangle \Delta x = 0$$

if

$$\langle m_i \rangle = 0 \quad \text{all } i.$$

The variance is

$$\langle \tilde{v}^2 \rangle = \sum_i \sum_j S(x_i)S(x_j)\langle m_i m_j \rangle (\Delta x)^2$$

Now assume m_i and m_j independent of $i \neq j$, so

$$\langle m_i m_j \rangle = \begin{cases} \langle m_i^2 \rangle & i = j \\ 0, & i \neq j \end{cases} .$$

Then

$$\langle \tilde{v}^2 \rangle = \sum_i S(x_i)^2 \langle m_i^2 \rangle (\Delta x)^2 .$$

Assume M is stationary, so m_i^2 is a constant, $\langle m^2 \rangle$.

Then

$$\langle v^2 \rangle = \langle m^2 \rangle (\Delta x)^2 \sum_i S(x_i)^2 .$$

We can replace $\Delta x \sum_i S(x_i)^2$ by $\int_a^b S(x)^2 dx$ if Δx is small enough, so

$$\langle \tilde{v}^2 \rangle = \langle m^2 \rangle \Delta x \int_a^b S(x)^2 dx .$$

Hence

$$D(v) = D(m) \sqrt{\Delta x \int_a^b S(x)^2 dx} . \quad (A-18)$$

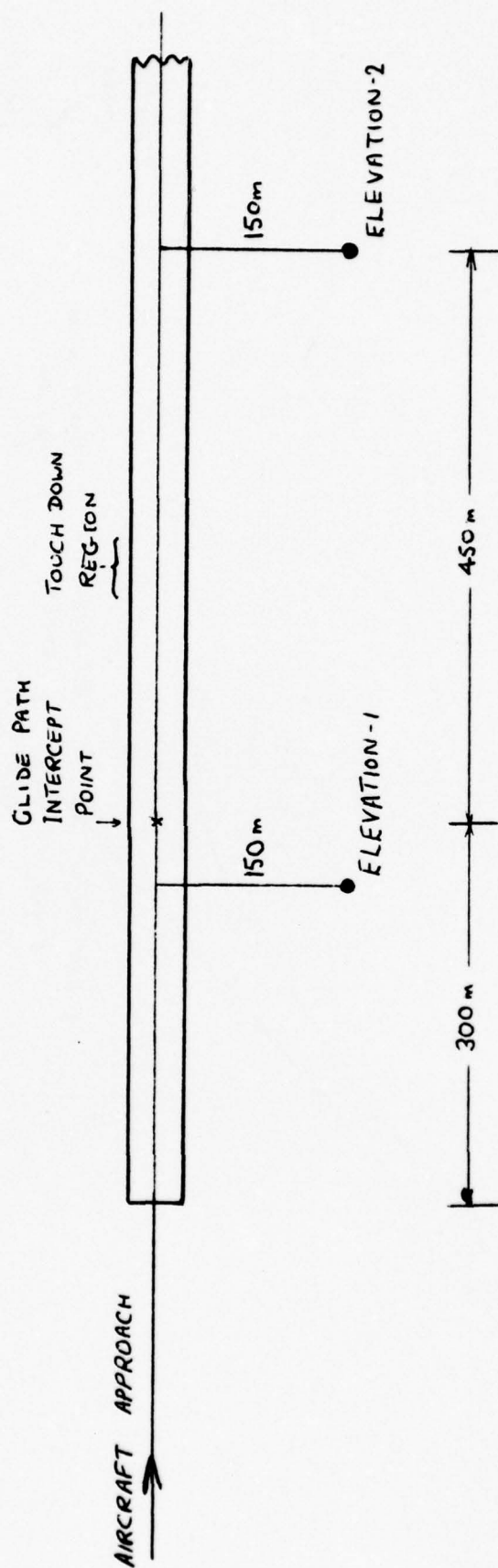


Fig.1

Fig.1 Airfield layout, with simulated antenna positions

Fig.2

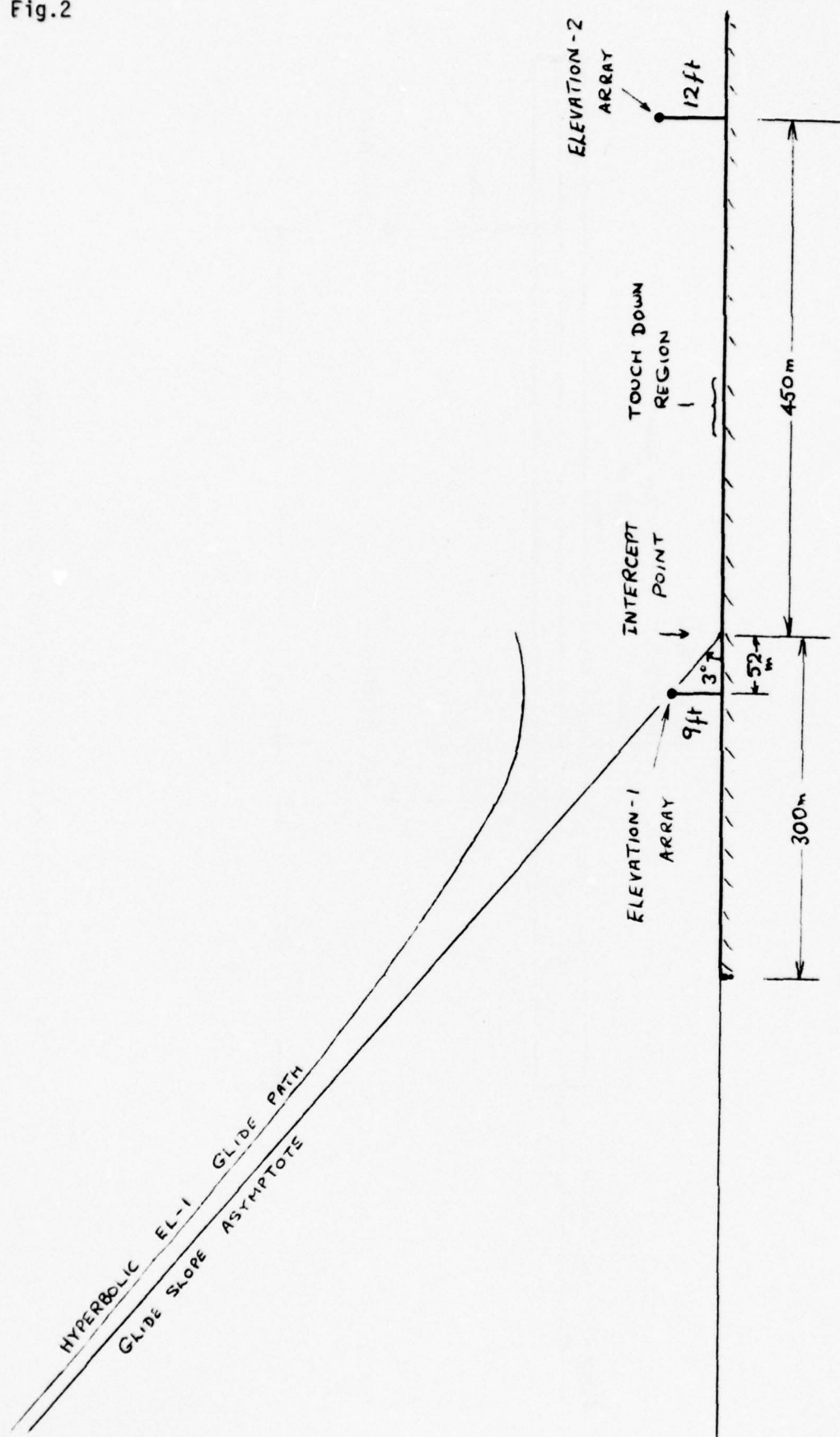


Fig.2 Approach geometry, vertical plane

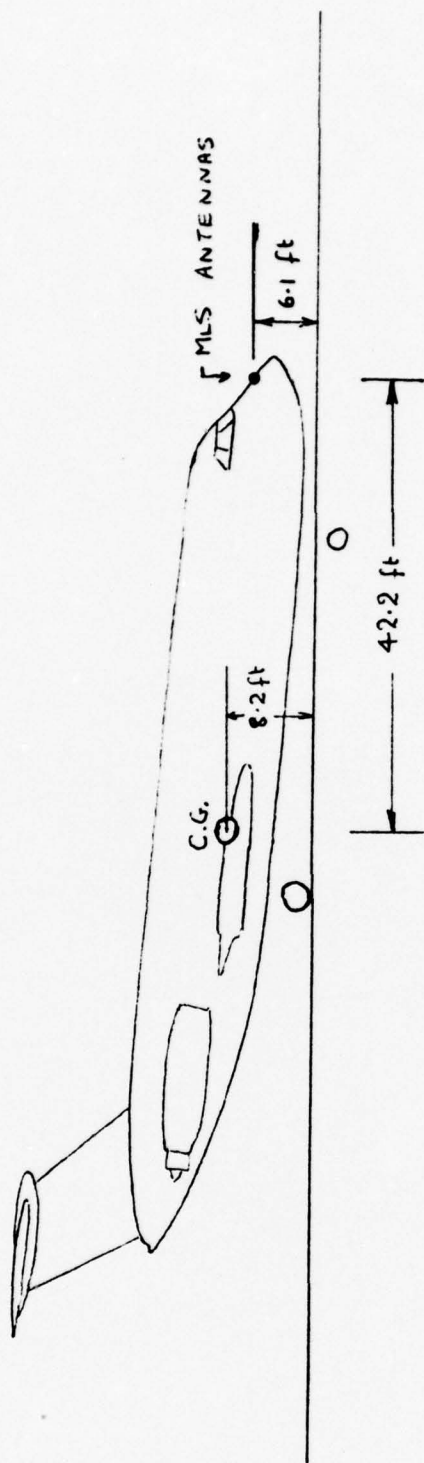


Fig.3

Fig.3 Disposition of MLS antennas on BAC 1-11 aircraft in nominal approach attitude

Fig.4

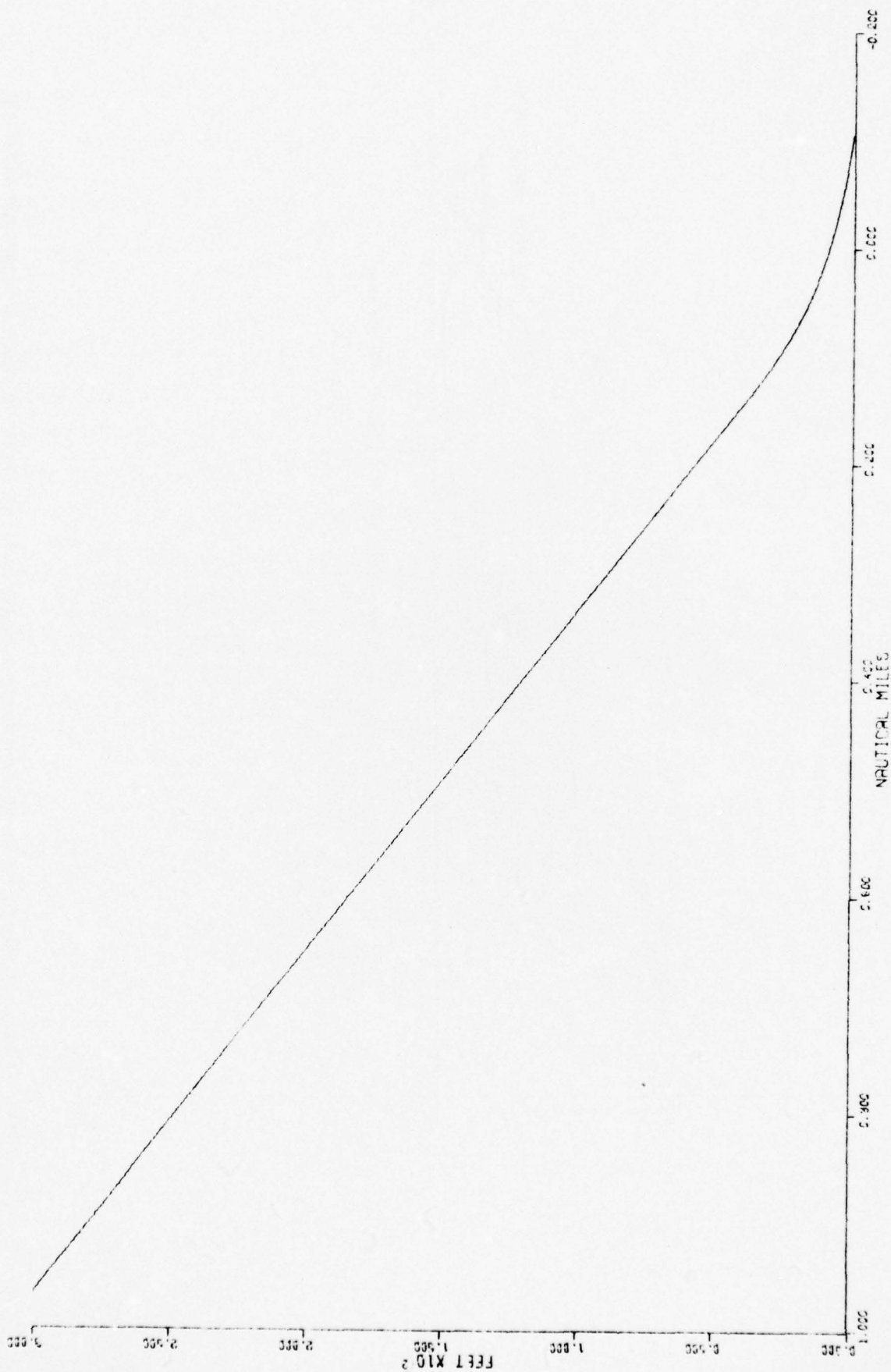


Fig.4 BAC 1-11 simulated MLS approach - wheel height versus range

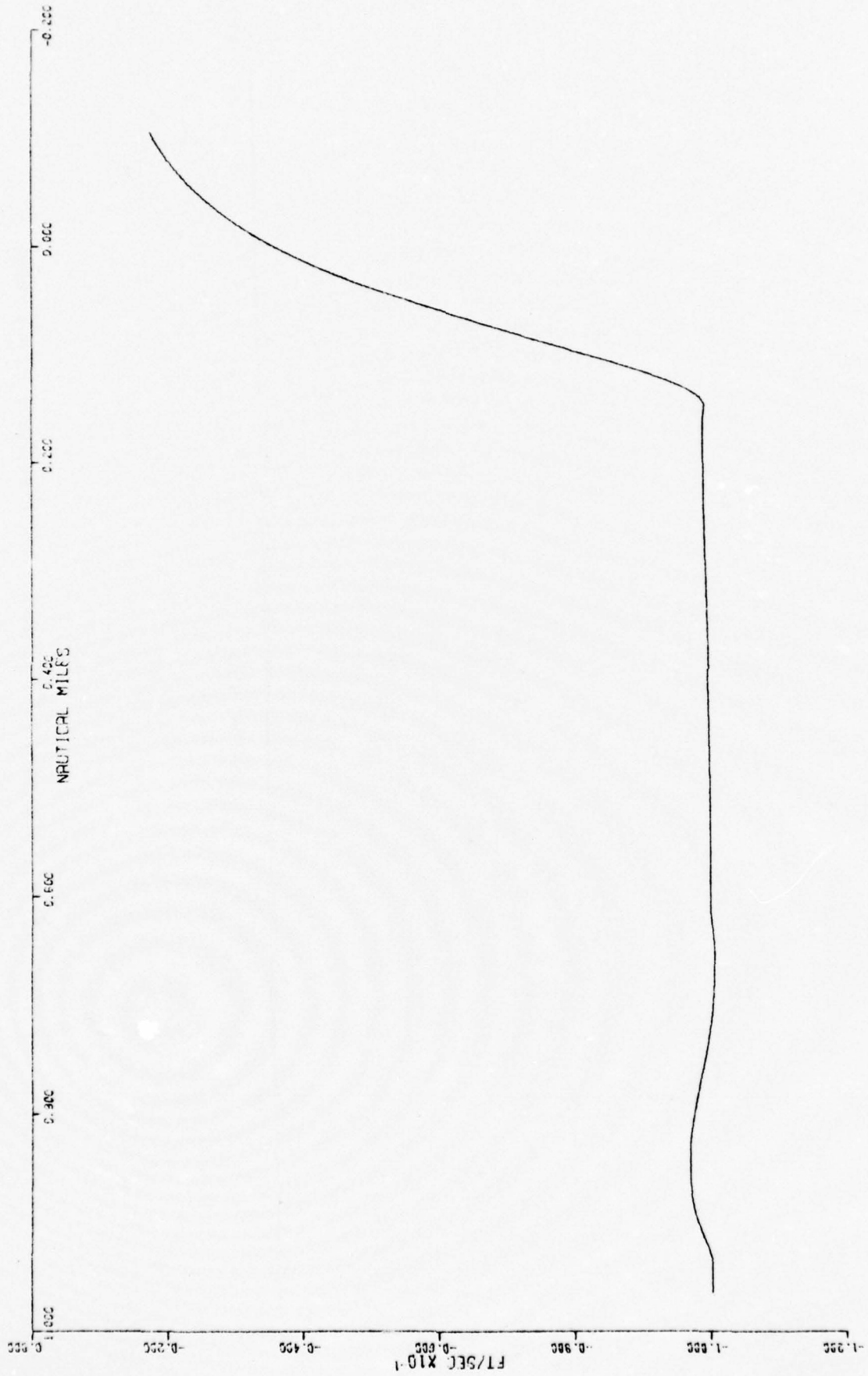


Fig.5

Fig.5 BAC 1-11 simulated MLS approach - rate of descent versus range

Fig.6

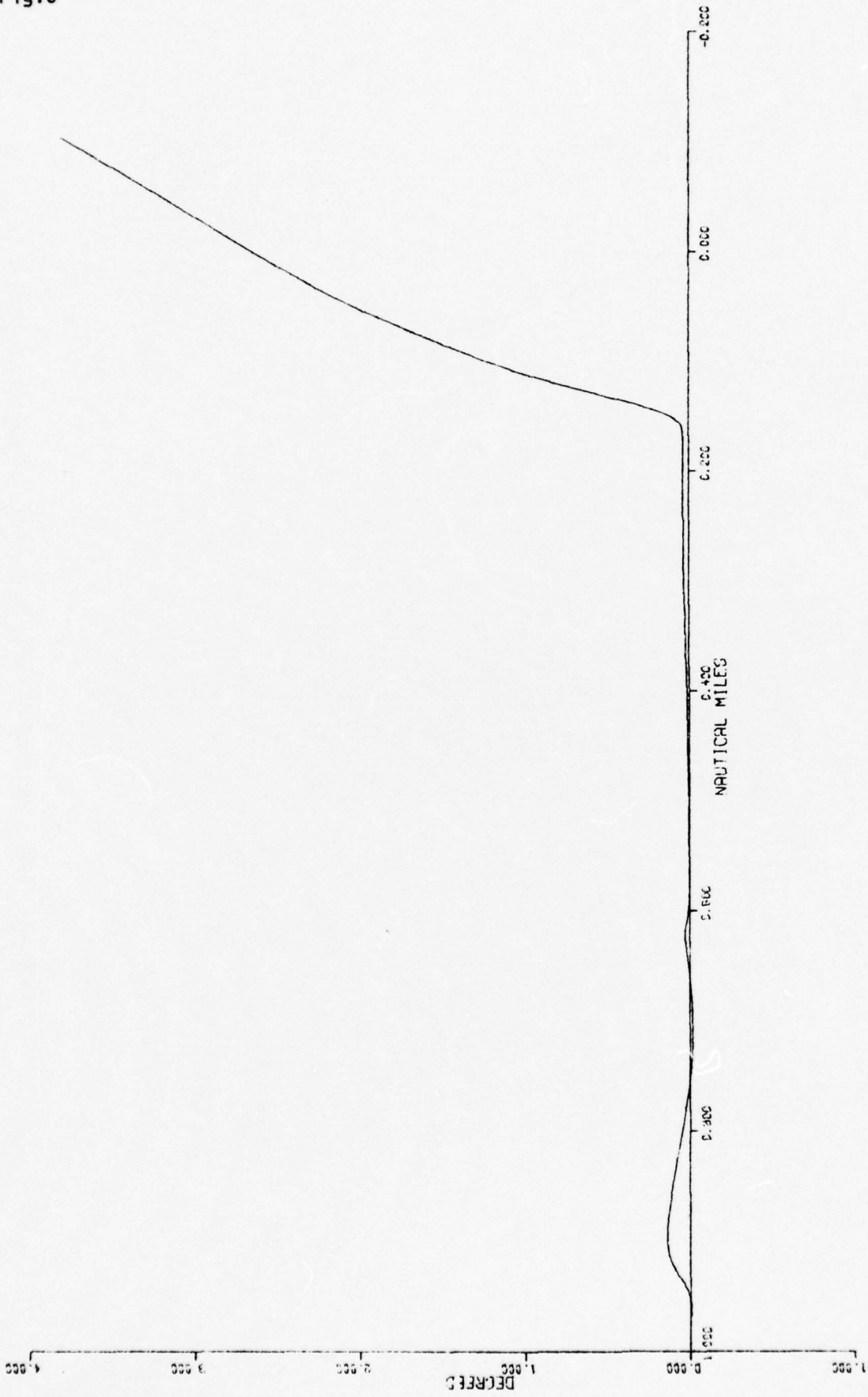


Fig.6 BAC 1-11 simulated MLS approach - pitch attitude versus range

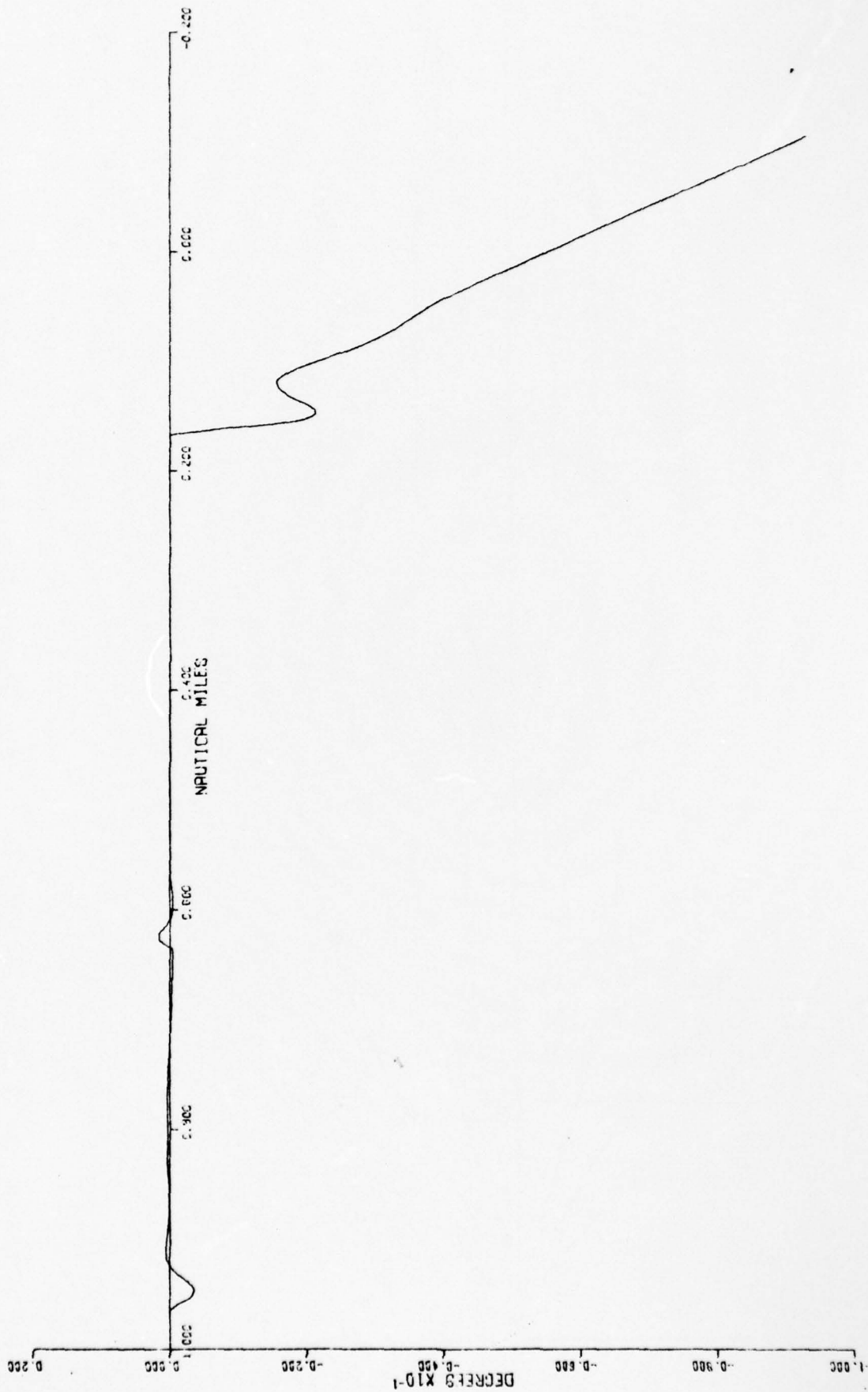


Fig.7

Fig.7 BAC 1-17 simulated MLS approach - elevator deflection versus range

Fig.8

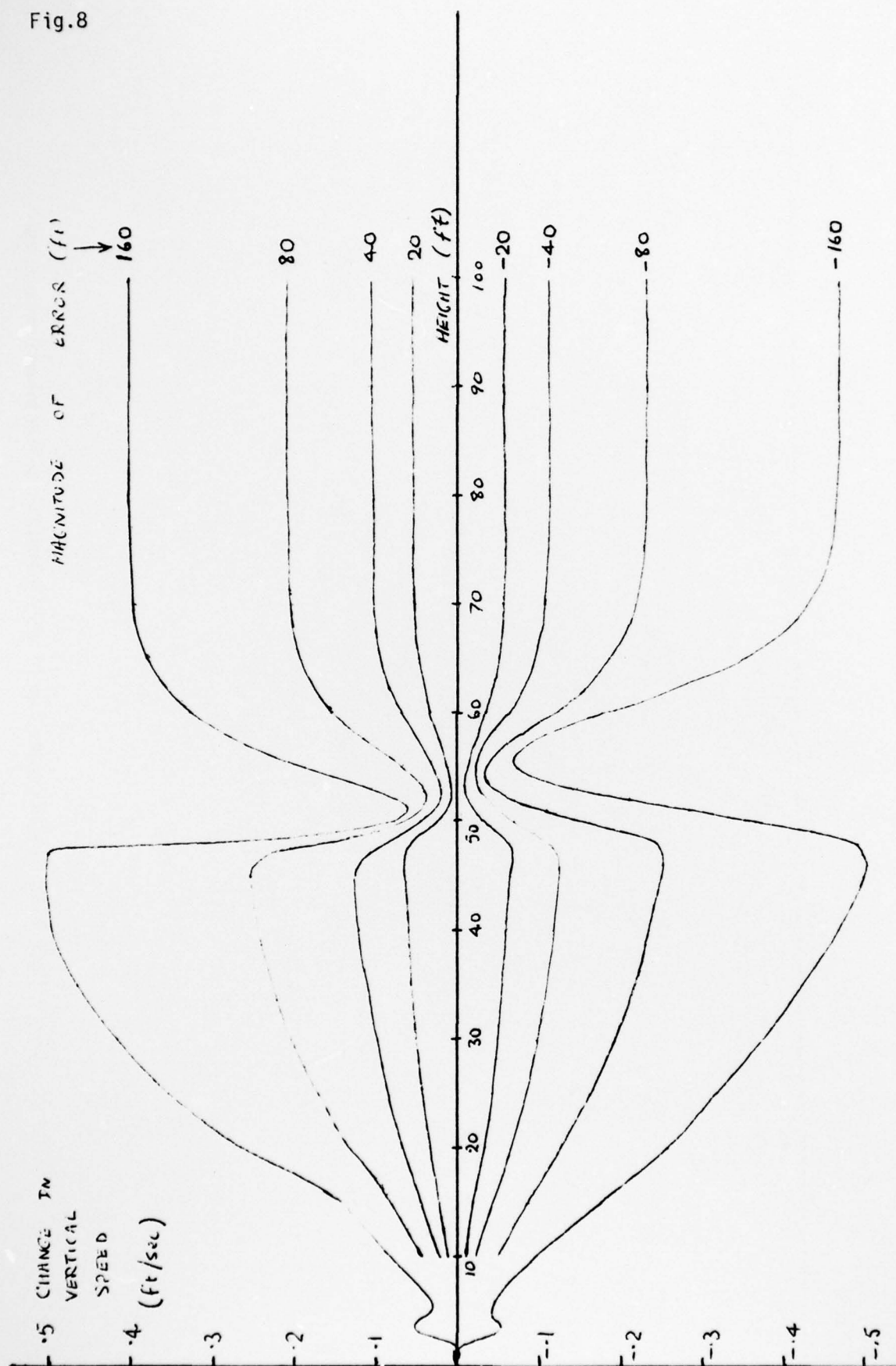


Fig.8 Change in rate of descent at touch-down due to a step error in range, versus height at which error begins

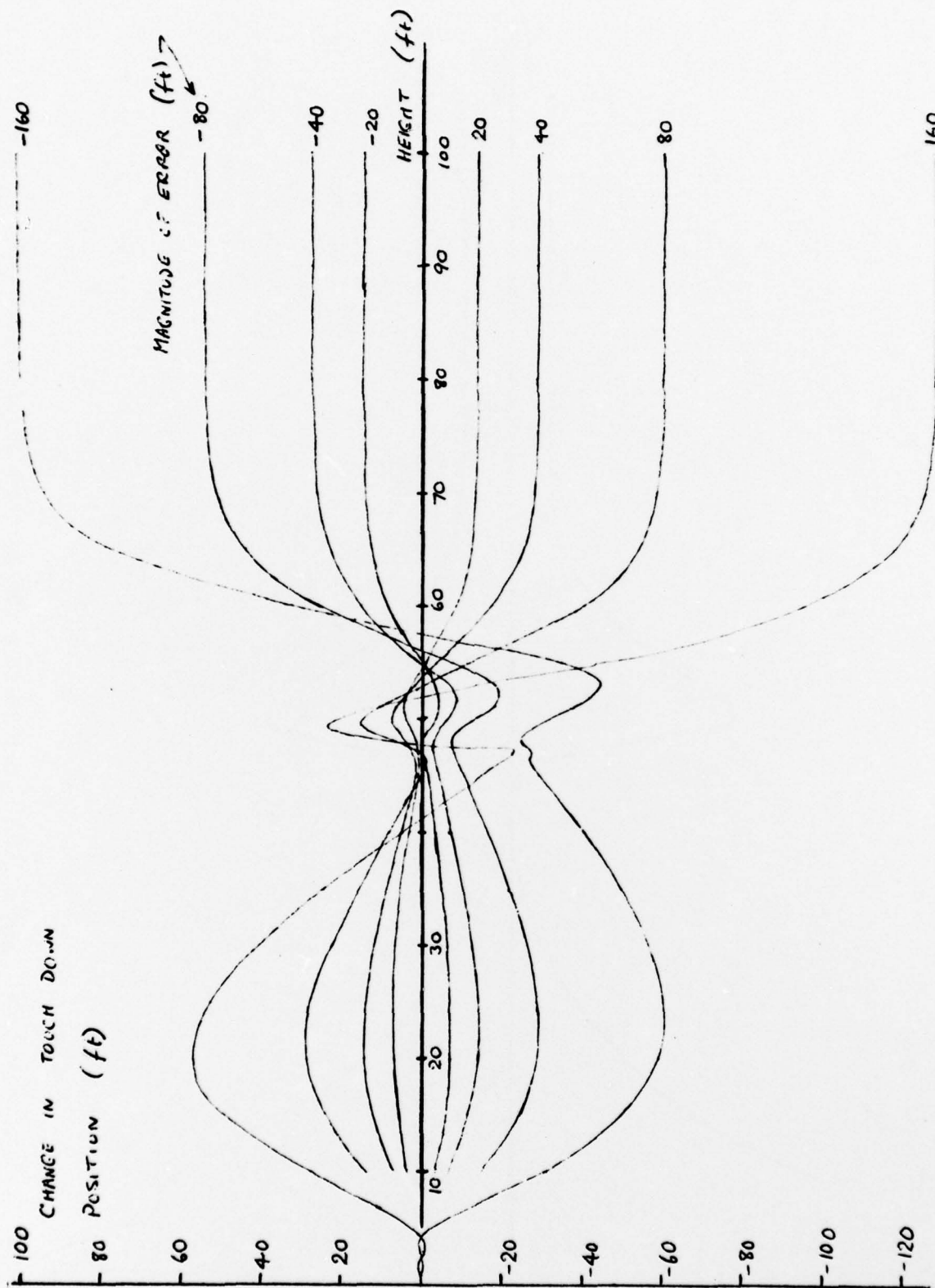


Fig.9 Change in touch-down position due to a step error in range, versus height at which error begins

Fig.10

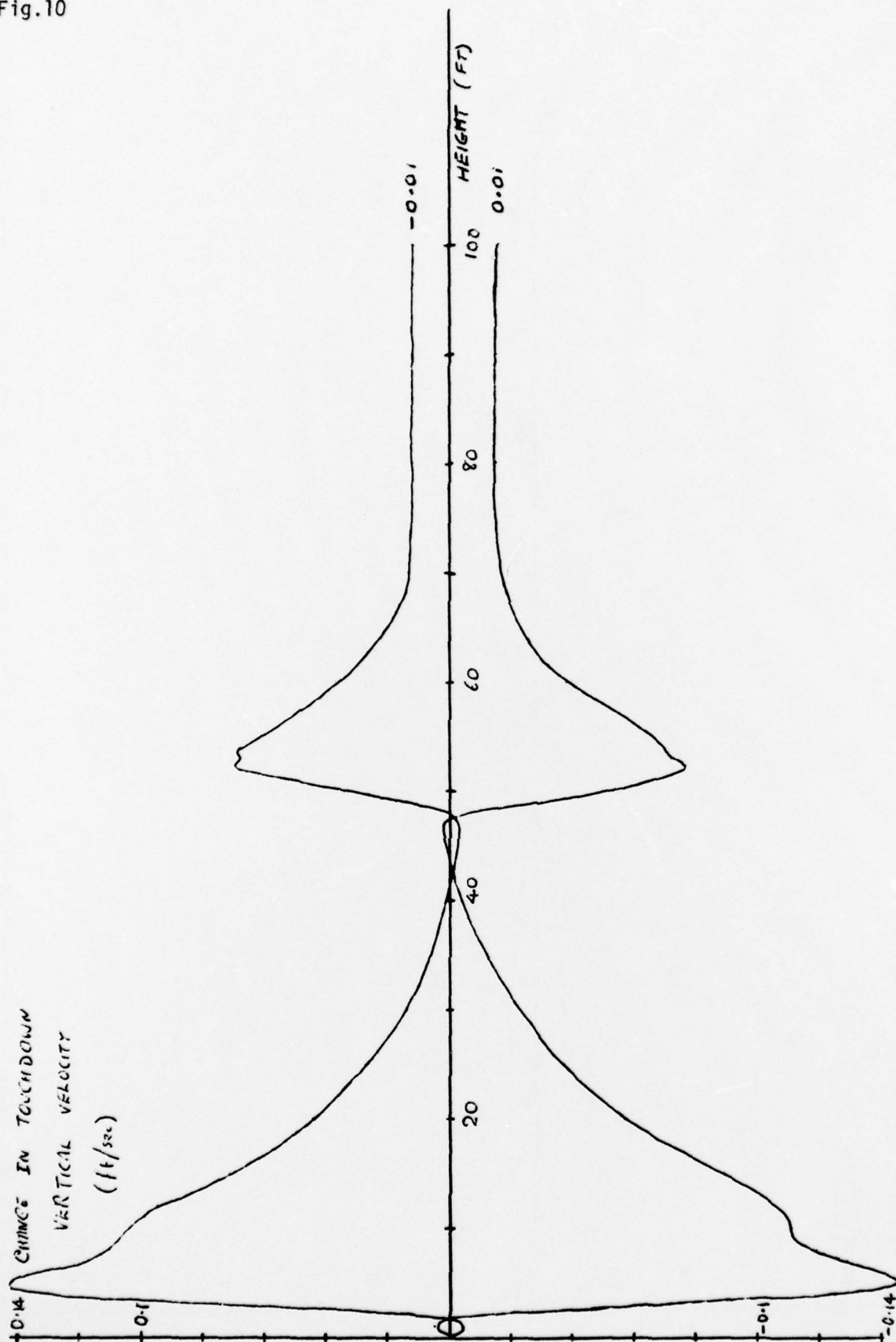


Fig.10 Change in vertical speed at touch-down due to a step error in angle versus height at which error begins

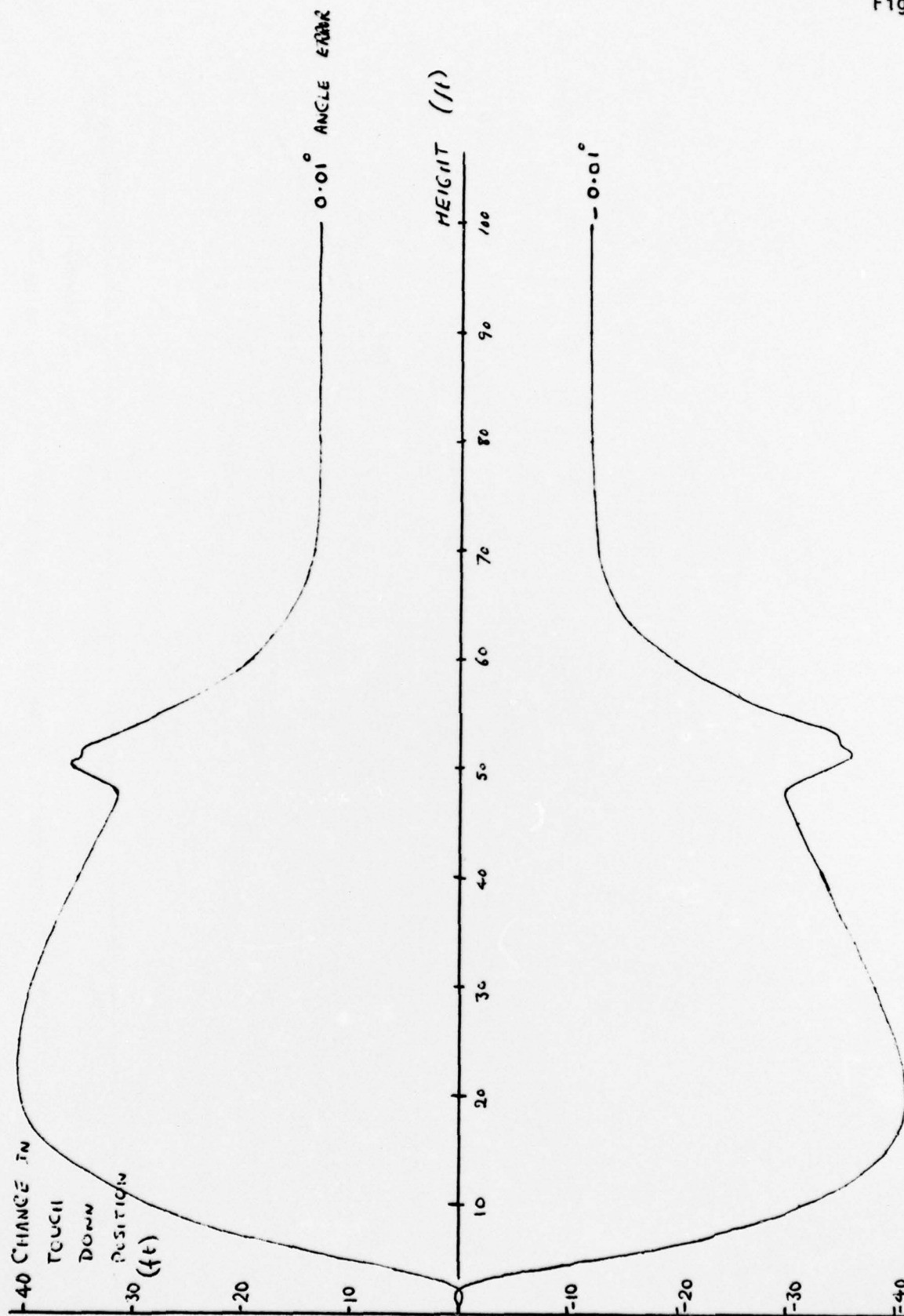


Fig.11

Fig.11 Change in touch-down position due to a step error in angle, versus height at which error begins

Fig.12

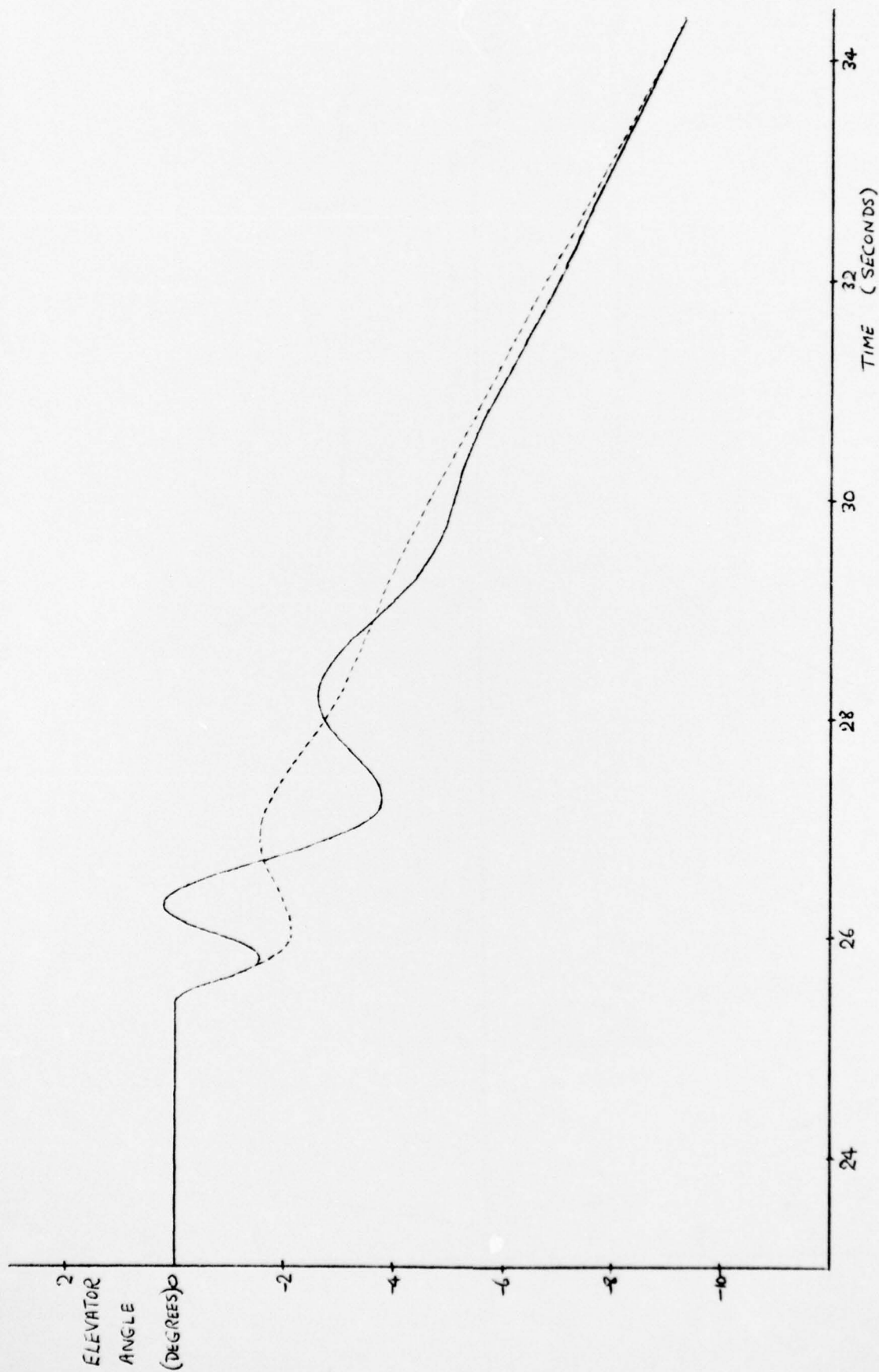


Fig.12 Elevator motion following a 100ft step error in range below 45ft

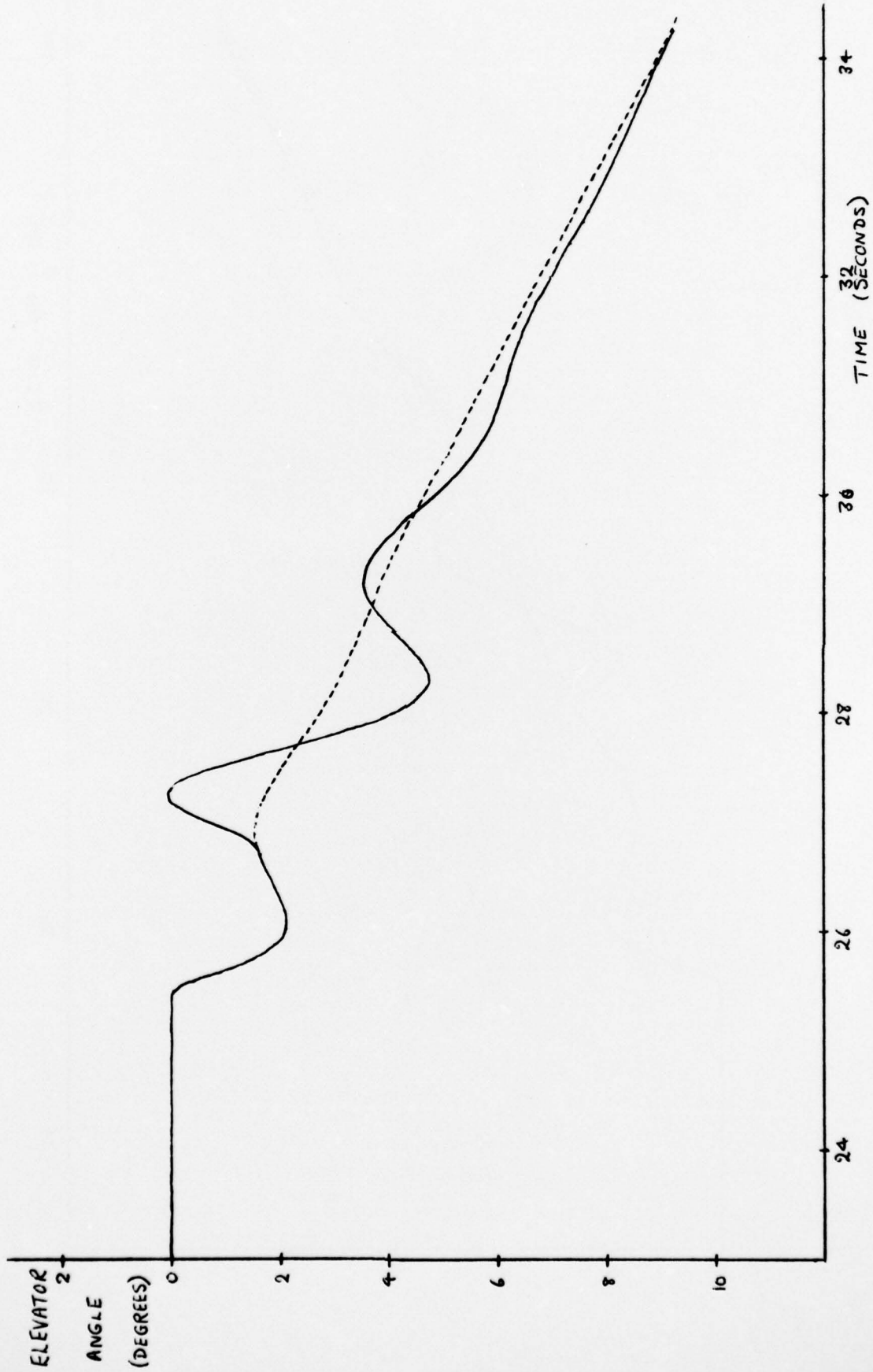


Fig.13

Fig.13 Elevator motion following 100ft step error in range at 35ft

Fig.14

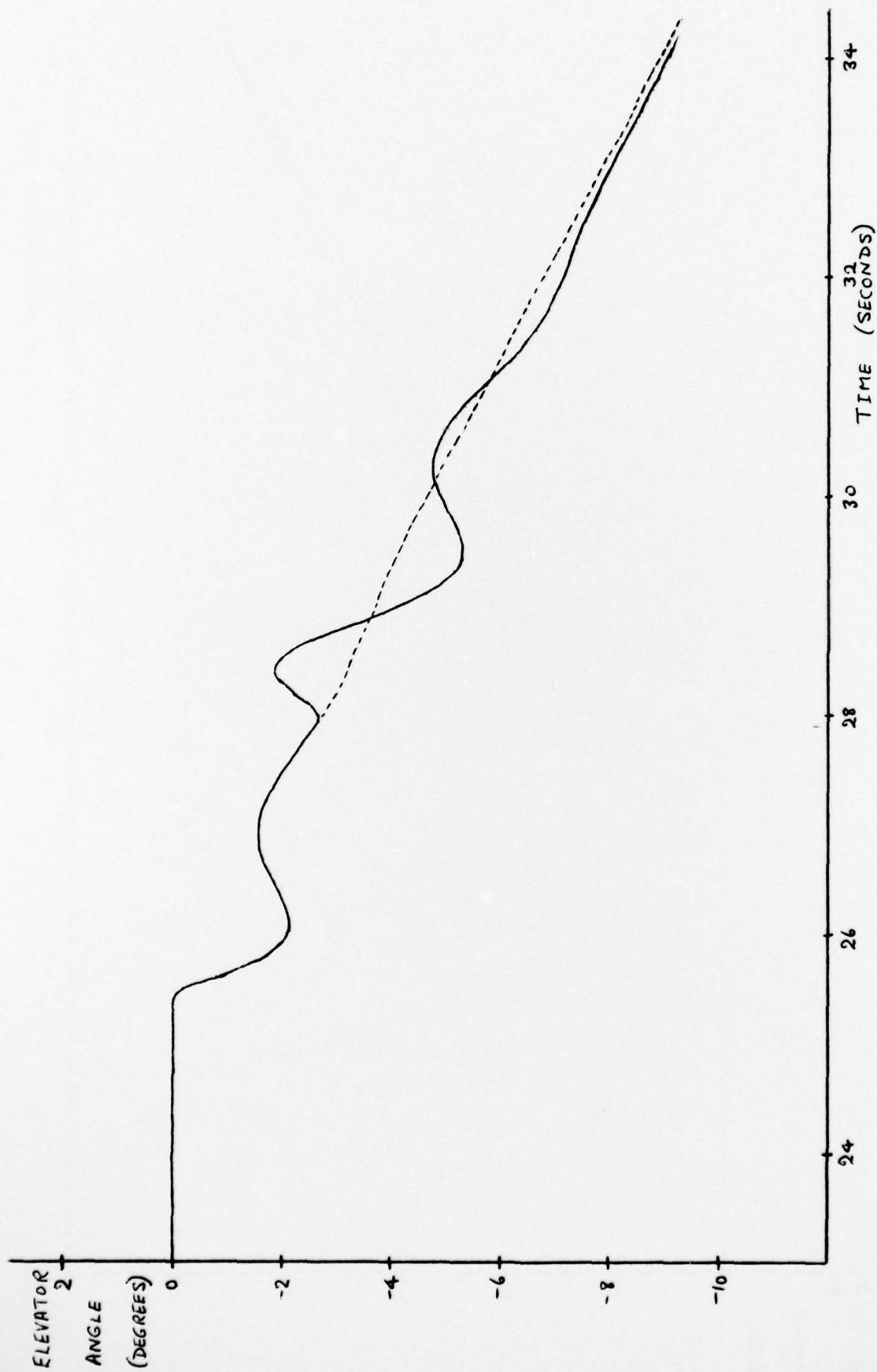


Fig.14 Elevator motion following a 100ft step error in range at 25ft

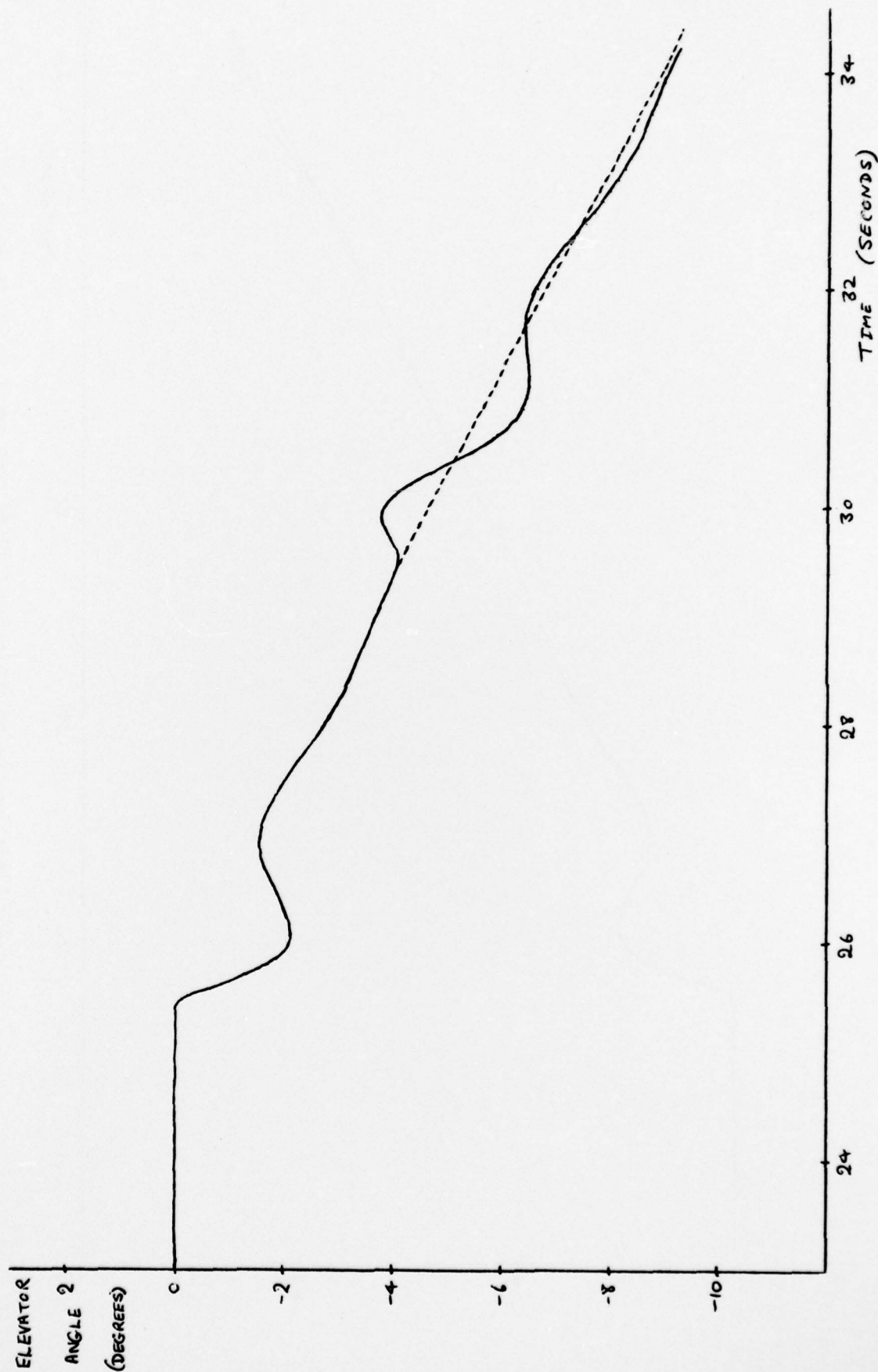


Fig.15

Fig.15 Elevator motion following a 100ft step error in range below 15ft

Fig.16



Fig.16 Elevation motion following a 100ft step error in range below 5ft

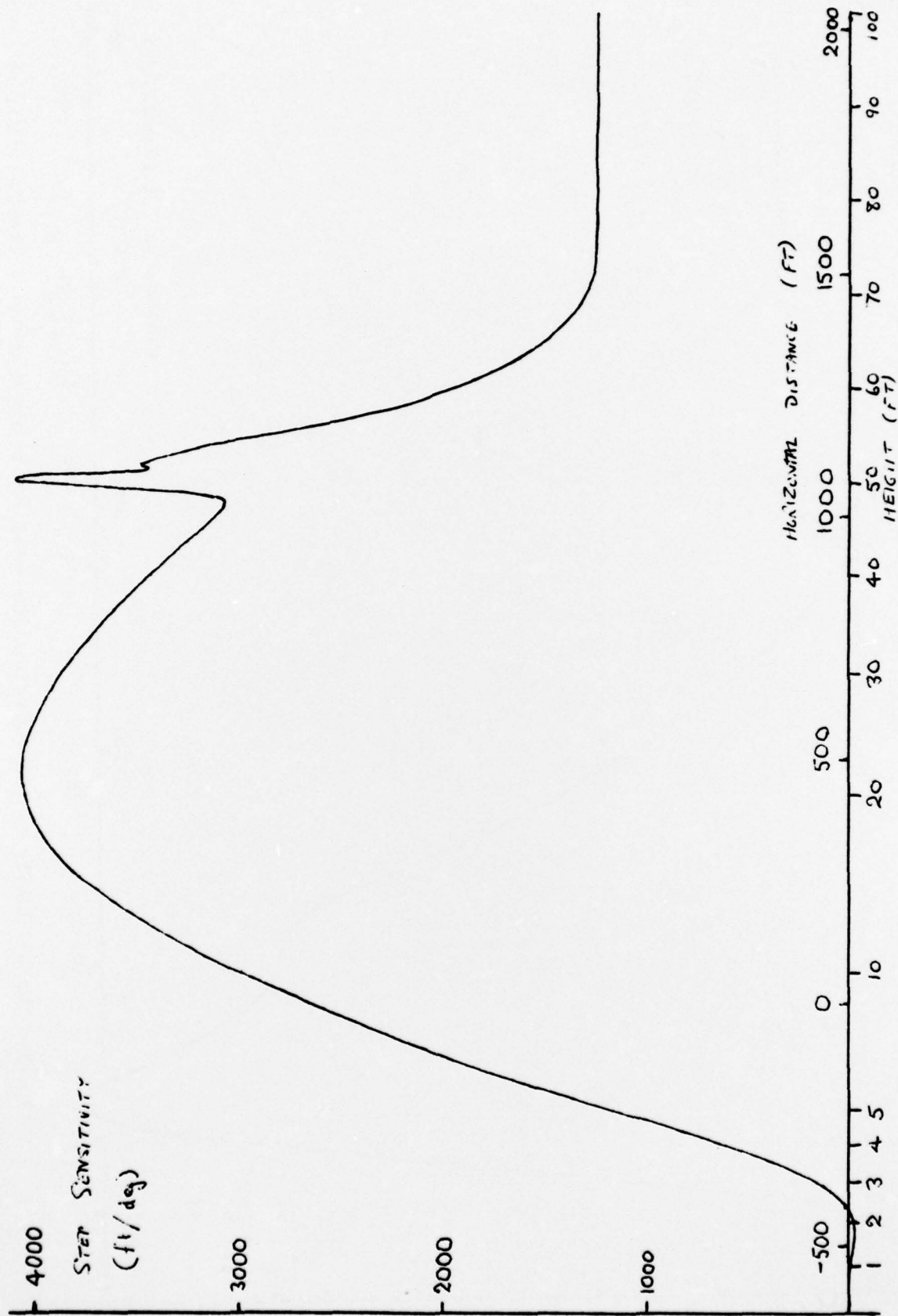


Fig.17

Fig.17 Step down sensitivity of touch-down position to angle versus horizontal distance

Fig.18

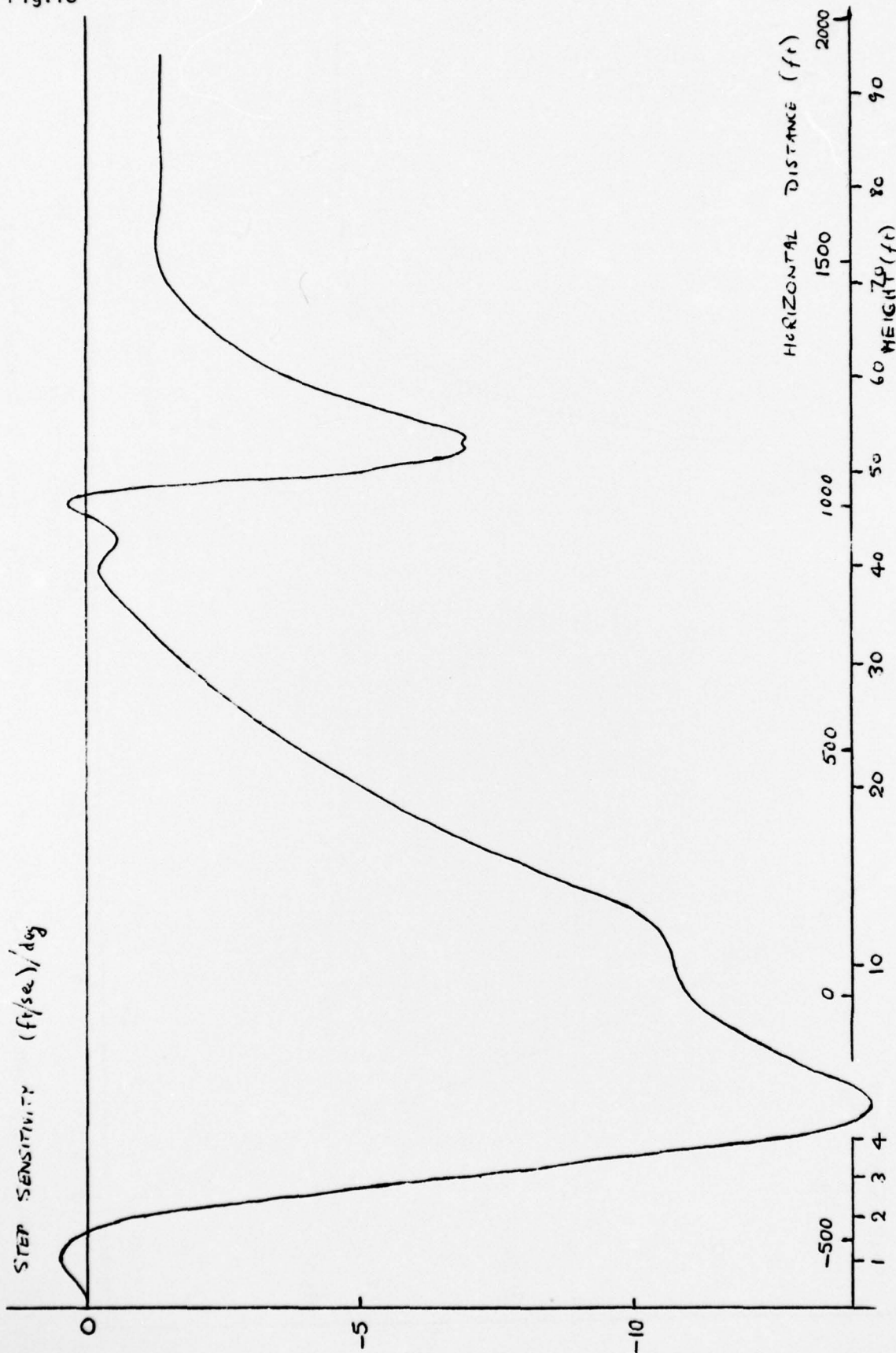


Fig.18 Step sensitivity of touch-down vertical velocity to angle versus horizontal distance

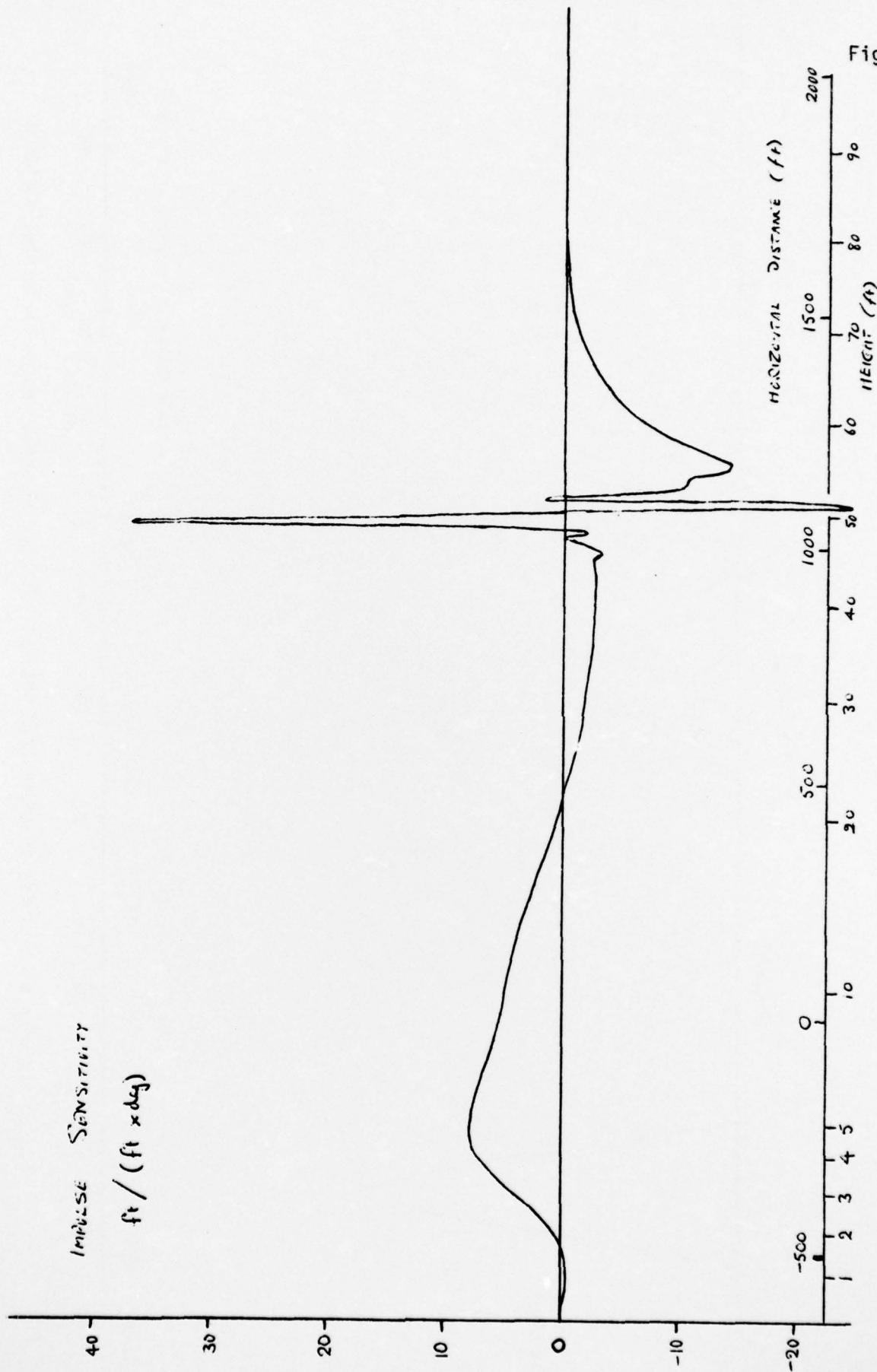


Fig.19

Fig.19 Impulse sensitivity of touch-down position to angle versus horizontal distance

Fig.20

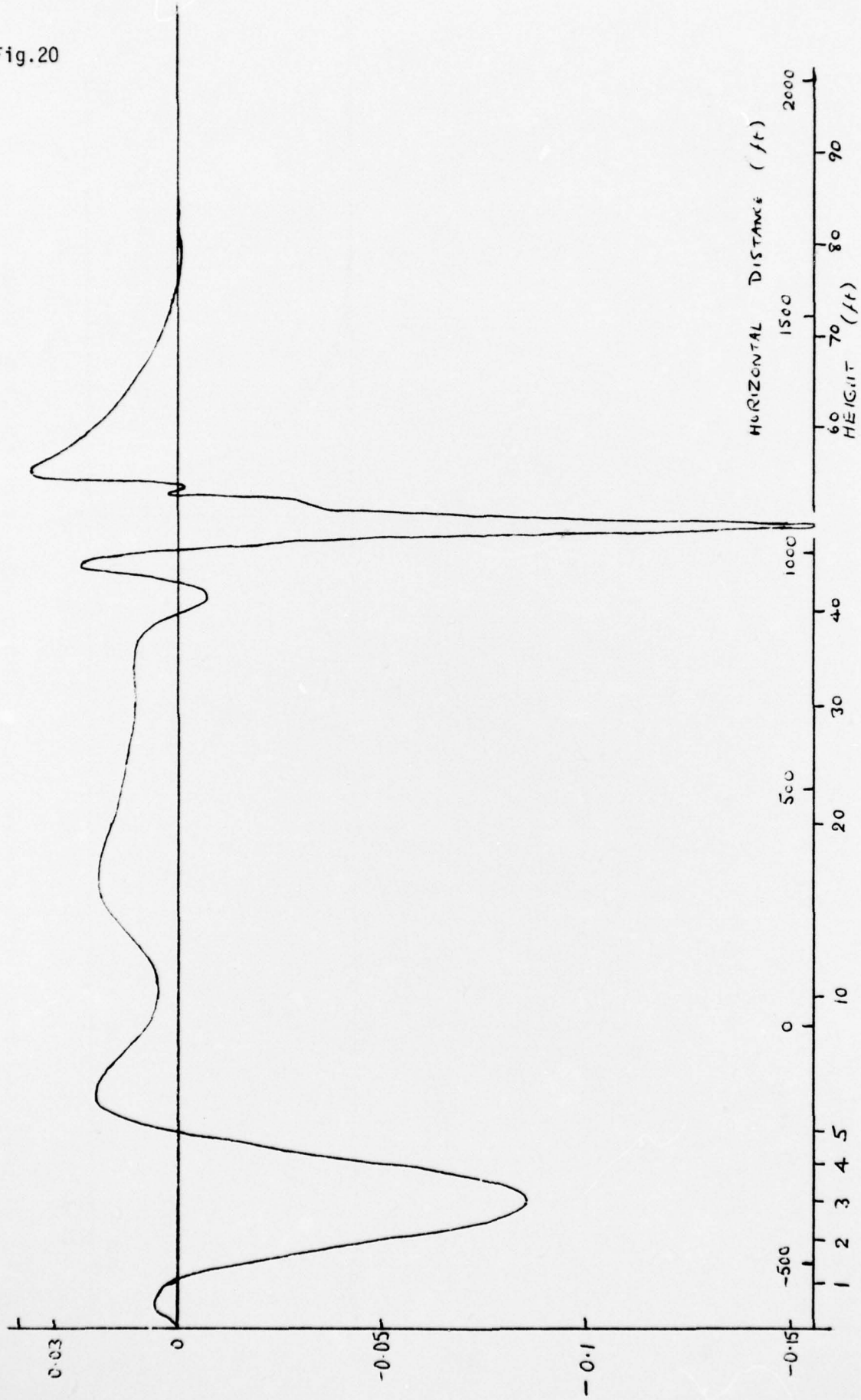


Fig.20 Impulse sensitivity of touch-down velocity to angle versus horizontal distance

Fig.21

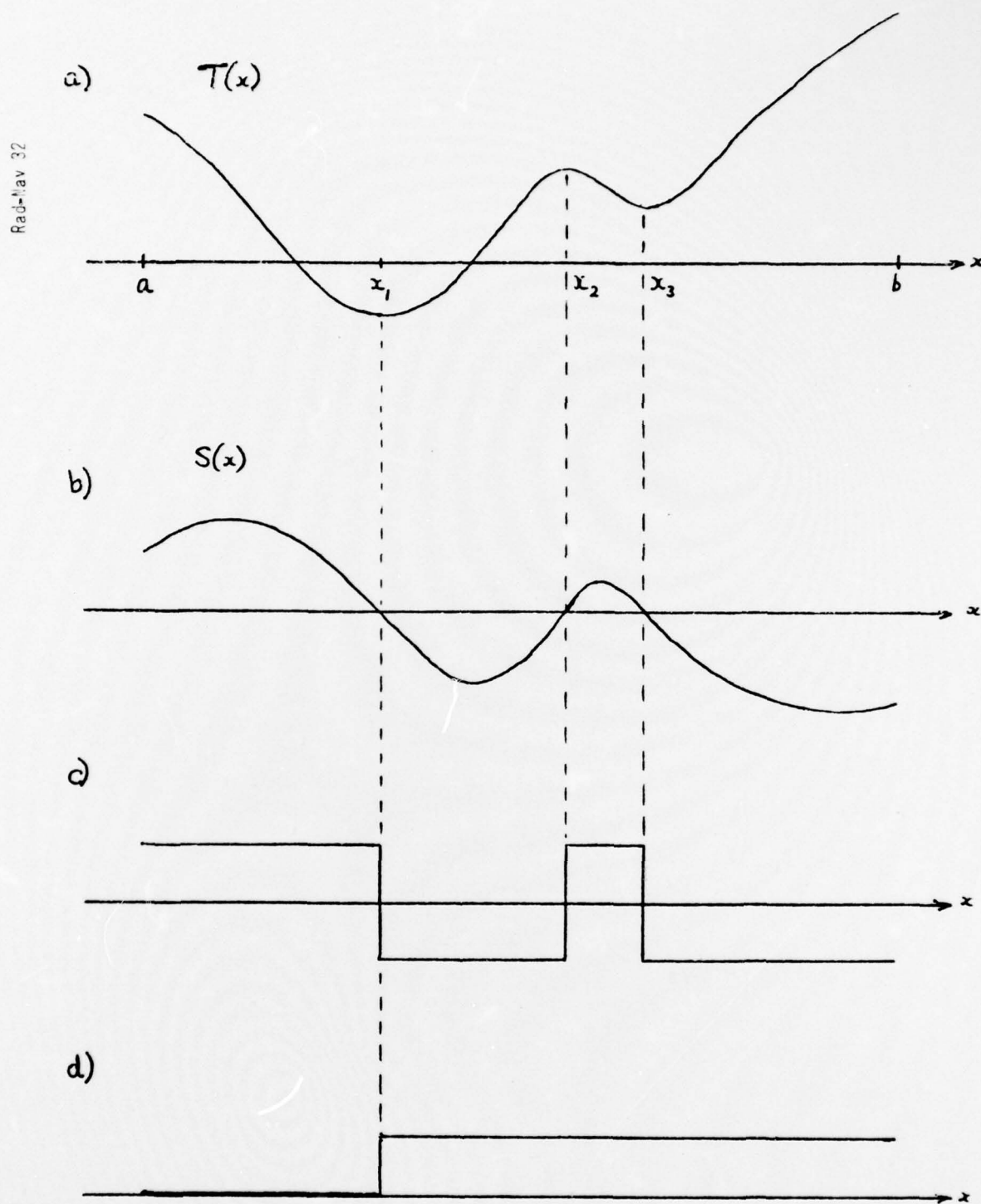


Fig.21 Illustrating the Appendix

REPORT DOCUMENTATION PAGE

Overall security classification of this page

UNCLASSIFIED

As far as possible this page should contain only unclassified information. If it is necessary to enter classified information, the box above must be marked to indicate the classification, e.g. Restricted, Confidential or Secret.

1. DRIC Reference (to be added by DRIC)	2. Originator's Reference RAE TM Rad-Nav 32	3. Agency Reference N/A	4. Report Security Classification/Marking UNCLASSIFIED		
5. DRIC Code for Originator 850100	6. Originator (Corporate Author) Name and Location Royal Aircraft Establishment, Farnborough, Hants, UK				
5a. Sponsoring Agency's Code N/A	6a. Sponsoring Agency (Contract Authority) Name and Location N/A				
7. Title Microwave landing system accuracy requirements for automatic flare-out.					
7a. (For Translations) Title in Foreign Language					
7b. (For Conference Papers) Title, Place and Date of Conference					
8. Author 1. Surname, Initials James, P.W.	9a. Author 2	9b. Authors 3, 4	10. Date March 1976	Pages 39	Refs. 1
11. Contract Number N/A	12. Period N/A	13. Project Doppler MLS	14. Other Reference Nos.		
15. Distribution statement (a) Controlled by - DRASA (b) Special limitations (if any) - Nil					
16. Descriptors (Keywords) (Descriptors marked * are selected from TEST) Microwave landing system. Flare guidance. Automatic flight control elevation guidance, distance measuring equipment.					
17. Abstract The report describes adaptation of a computer based simulation of a transport aircraft automatic landing system to enable study of microwave landing system (MLS) flare guidance. The simulation was used to examine the allowable errors from the range and elevation angle measuring sub-systems of the MLS flare system.					

FS910/1